Alpha cells dedifferentiate and then transdifferentiate into delta cells during the progression of autoimmunity in non-diabetic NOD mice.

METHODS

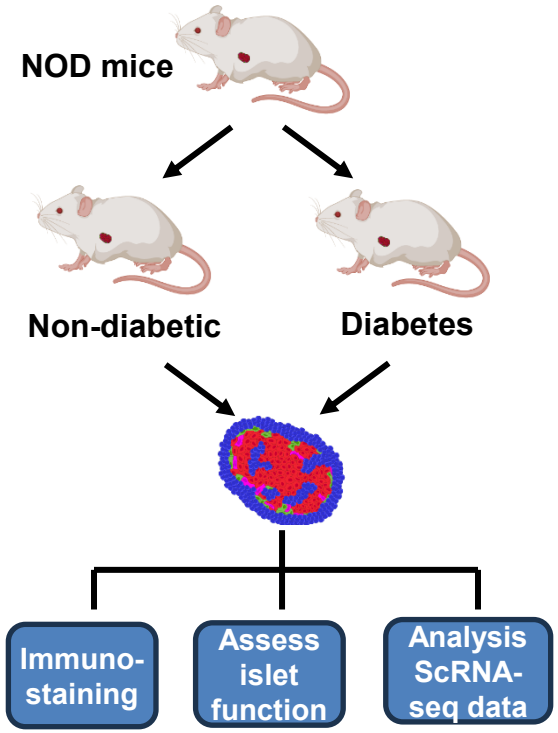

OUTCOME

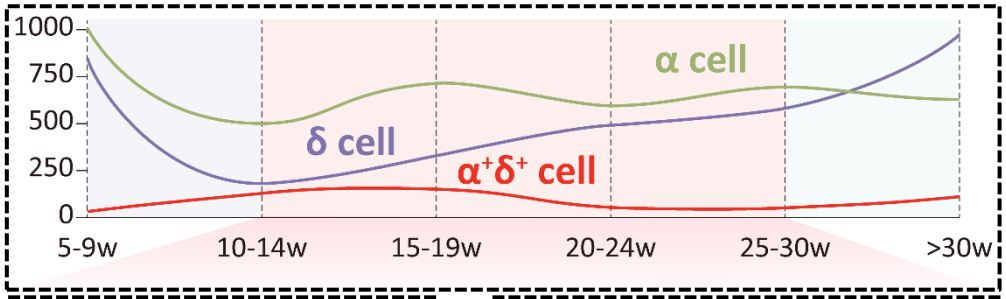

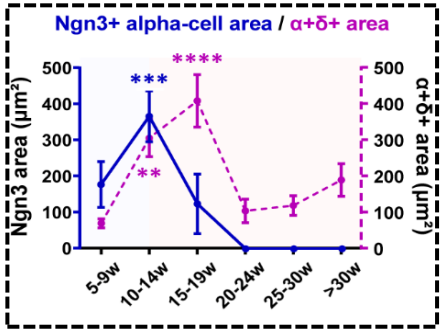

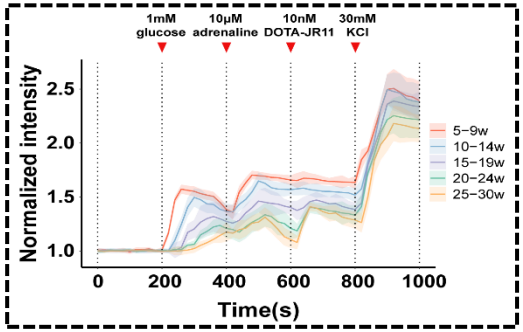

CONCLUSION

Alpha cells transdifferentiate into delta cells, and the increased delta cells and somatostatin inhibits glucagon secretion during the progression of autoimmunity in non-diabetic NOD mice.

Alpha cells transdifferentiate into delta cells during the progression of autoimmunity in non-diabetic NOD mice

Zhehui Li[1], Xinyun Wu[1], Qi Kang[1], Qi Ren[1], Yi Zhang[1], Yi Zhang[2], Quanwen Jin[1], F. Susan Wong[3*], Mingyu Li[1,4*]

[1]State Key Laboratory of Cellular Stress Biology and Fujian Provincial Key Laboratory of Innovative Drug Target Research, School of Pharmaceutical Sciences and School of Life Sciences, Xiamen University, Xiamen 361102, China

[2]Department of Endocrinology, Quanzhou First Hospital Affiliated to Fujian Medical University, Quanzhou 362000, China

[3]Division of Infection and Immunity, Cardiff University School of Medicine, Cardiff CF14 4XN, UK

[4]State Key Laboratory of Vaccines for Infectious Diseases, Xiang An Biomedicine Laboratory, Xiamen University, Xiamen 361102, China

Running head: Alpha cells convert into delta cells in NOD mice

* Correspondence:

Mingyu Li PhD.

Fujian Provincial Key Laboratory of Innovative Drug Target Research, School of Pharmaceutical Sciences, Xiamen University, Xiamen 361102, China.

Phone: (+86) 592-2182453, Email: limingyu@xmu.edu.cn

F. Susan Wong FRCP, PhD.

Division of Infection and Immunity, Cardiff University School of Medicine, Cardiff

CF14 4XN, UK, Phone: (+44) 29206 87000, E-mail: WongFS@cardiff.ac.uk

Abstract

The incidence of Type 1 diabetes (T1D) has increased in recent years. Although extensive research has focused on immune damage to insulin-producing beta cells, the pathophysiological effects on other endocrine cells within pancreatic islets remain less well-documented. This study investigates the changes in the number and proportion of alpha-, beta- and delta- cells, as well as hormone secretion, during the progression of autoimmunity in non-diabetic non-obese diabetic (NOD) mice at different ages. Our findings reveal significant heterogeneity in islet size, endocrine cell composition and degree of immune infiltration. We propose a novel classification system for islet subtypes based on this observed heterogeneity. Notably, we noticed an age-related increase in delta cells in older non-diabetic NOD mice. Additionally, we observed an increase in glucagon and somatostatin double-positive cells following immune cell infiltration in non-diabetic mice. Our further analysis demonstrated that these double-positive cells represent a transdifferentiation process from alpha cells to delta cells, mediated by an alpha-cell dedifferentiation intermediate. Moreover, our results indicated that the increased presence of delta cells and somatostatin in pancreatic islets significantly inhibits alpha cell function during the progression of autoimmunity. Thus, our findings provide valuable insights into the dynamic changes in alpha and delta cells throughout the natural history of T1D.

Keywords: Alpha cell transdifferentiation; Delta cells; Islet heterogeneity; NOD mice; Type 1 diabetes.

New & Noteworthy:

The NOD mouse, is widely used as an T1D animal model. Although the mice have the same genetic background, approximately 20% of female NOD mice do not develop diabetes. In this study, we reveal that alpha cells dedifferentiate and then transdifferentiate into delta cells during the progression of autoimmunity in non-diabetic NOD mice. The increased delta cells secrete more somatostatin which inhibits alpha cell secretion of glucagon, thereby potentially attenuating the increase in blood glucose levels in these mice.

1. Introduction

Type 1 diabetes (T1D) is an autoimmune disorder characterized by the immune-mediated destruction of pancreatic beta cells, resulting in reduced insulin secretion (1). To date, T1D treatment has predominantly centered on insulin therapy, with numerous studies focusing on beta cell dysfunction. In addition to insufficient insulin production, elevated circulating glucagon levels have been observed both postprandially and at rest in individuals with T1D (2-4). However, a subset of individuals with T1D experience severe hypoglycemia following insulin administration due to impaired glucagon responses (5). These observations suggest that both insulin deficiency and dysregulation of glucagon release and function contribute to the pathophysiology of T1D. While several studies have reported changes in alpha cells in NOD mice, the findings regarding changes in alpha cell mass remain controversial. Pechhold et al. observed a decrease in alpha cell mass in diabetic NOD mice (6), whereas others have noted an increase (7, 8). These discrepancies may arise from differences in the time points chosen for observation.

Regarding delta cells in NOD mice, both the proportion and mass of delta cells increase during T1D progression (7, 9). This increase has also been observed in individuals with T1D (10). Moreover, one previous study has documented an approximately 30% increase in fasting circulating somatostatin levels in individuals with T1D (11). In addition, delta cells secrete more somatostatin in inflammatory environments and, in the absence of beta cells, inhibit alpha cell glucagon secretion (12). Thus, although less frequently addressed in previous studies, delta cells may play a significant functional role in T1D. However, the underlying mechanisms driving this delta cell expansion remain unclear.

The non-obese diabetic (NOD) mouse, known for spontaneously developing

T1D, is widely used as an animal model of T1D (13, 14). Female NOD mice begin exhibiting symptoms of diabetes as early as 12 weeks of age, with increasing incidence of hyperglycemia and T1D as they age, reaching a lifetime incidence of approximately 80% (15). However, approximately 20% of female NOD mice do not develop hyperglycemia before 35 weeks of age and are unlikely to progress to diabetes, exhibiting distinct islet characteristics compared to other mice (16).

To gain a more comprehensive understanding of the dynamic changes in alpha and delta cells during autoimmunity progression and the potential mechanisms driving these changes in non-diabetic NOD mice, we conducted a quantitative analysis of alpha, beta, and delta cells in the islets of non-diabetic NOD mice across six age groups (5 to 32 weeks). Our results indicate that alpha cell mass remains relatively stable, while delta cell mass increases during autoimmunity progression. Furthermore, alpha-to-delta cell transdifferentiation appears to be the primary driver of delta cell expansion in non-diabetic NOD. These newly increased delta cells, in turn, inhibit the response of alpha cells to hypoglycemic stimuli.

2. Materials and Methods

2.1 Mice

NOD mice were bred and maintained at the Xiamen University Experimental Animal Center. The animals were housed in individually-ventilated cages (≤ 5 mice per cage) within a specific pathogen-free facility with a 12- hour light-dark cycle at a temperature of 20-23 ℃. They were provided with standard chow and water ad libitum. By 32 weeks of age, the cumulative incidence of autoimmune diabetes in our female NOD mice reaches 81% (Fig. S1). All experimental procedures were approved

by the Animal Care and Use Committee of Xiamen University (Protocol No. XMULAC20220141).

2.2 Blood glucose monitoring

Female NOD mice were monitored weekly for glycosuria from 8 weeks of age. Upon detection of positive glycosuria using a blood glucose meter (Yuwell, China), diabetes was diagnosed when blood glucose levels exceeded 13.9 mmol/L (1), confirmed by a second measurement. Diabetic mice were euthanized via cervical dislocation on the same day of diagnosis, and pancreatic tissue samples were collected. The incidence of diabetes in our NOD mouse colony is illustrated in figure S1.

2.3 Pancreatic histological preparation and immunofluorescence staining

Whole pancreata were fixed in 4% paraformaldehyde. After infusion with 10% and 20% sucrose at 4℃, the tissues were embedded in OCT compound, snap-frozen and stored at -80℃ as previously described (17). Frozen sections were processed according to a standard protocol (18). Briefly, 6 μm-thick sections were incubated with primary antibodies overnight at 4℃, followed by incubation with secondary antibody for 2 hours at room temperature (RT). Images were captured using a Leica SP8 confocal microscope (Leica, Germany), and quantification was performed using ImageJ software (National Institutes of Health). Confocal images were first converted to 8-bit format and split into individual color channels. For each channel, thresholds were set using the "Auto Threshold" function to minimize background and normalize signal intensity across samples. Co-localization was assessed using the "Image Calculator" function with the "AND" operation to generate a mask of overlapping signals. Cells exhibiting overlapping signals for both glucagon and somatostatin were

134 defined as alpha-delta double-positive cells.

135 Primary antibodies used included: guinea pig anti-insulin (DAKO, A0564),
136 rabbit anti-glucagon (Abcam, ab92517), mouse anti-glucagon (Sigma-Aldrich,
137 G2654), rat anti-somatostatin (Abcam, ab30788), rat anti-somatostatin (Thermo
138 Fisher Scientific, MA5-16987), mouse anti-CD45 (Abcam, ab33923), mouse
139 anti-neurogenin3 (BD Biosciences, 610790), mouse anti-neurogenin3 (Santa Cruz
140 Biotechnology, Sc-374442), mouse anti-Sox9 (Proteintech Group, 67439-1-Ig), rabbit
141 anti-Aldh1a3 (Novus Biologicals, NBP2-15339), rabbit anti-Nkx6.1 (Abcam,
142 ab221549), and rabbit anti-Ki67 (Abcam, Ab15580).

143

144 **2.4 Pancreatic islet isolation**

145 The isolation of islet was performed as previously described (19). Following
146 euthanasia of mice, a buffer containing 1mg/mL type IV collagenase (Gibco,
147 17104019) was injected into the common bile duct. The pancreata were dissected and
148 incubated in a 37℃ water bath for 10 minutes, then gently shaken for approximately 5
149 minutes until complete digestion. The tissue was resuspended, and islets were purified
150 by density gradient centrifugation (Sigma, 10771). Individual islets were hand-picked
151 under a dissecting microscope and cultured in 4mL RPMI 1640 medium (Gibco,
152 C11875500) containing 10% FBS and 1% penicillin/streptomycin in a 37℃ incubator.
153 The purity of islet was assessed by dithizone solution, and the isolated islets with
154 purity up than 90% were used for experiments (Fig. S2).

155

156 **2.5 Measurement of islet hormone content**

157 Islets from three mice of each age group were pooled. Five islets from each
158 group were randomly selected and placed in 1.5mL centrifuge tubes. Pre-prepared

acidified ethanol (50 mL of 75% ethanol with 750 μL of concentrated hydrochloric acid) was added to each tube. Islets were homogenized and slowly shaken overnight at 4℃. Samples were then centrifuged at 4000 rpm for 30 minutes at 4℃, and the supernatant was collected and diluted 100-500 times for measurement of insulin, glucagon and somatostatin by ELISA (Meimian, China) according to the manufacturer's instructions.

2.6 Measurement of islet hormone secretion

Islets from three non-diabetic NOD mice in each age group were pooled and 20 islets from each group were randomly selected and cultured in 96-well plates either with or without the somatostatin receptor 2 inhibitor, 10nM DOTA-JR11, in RPMI 1640 medium. Hormone content in the supernatant was measured after culture for 2 hours and 24 hours, respectively.

2.7 Calcium imaging and quantification of cytosolic Ca^{2+} content

Islets from each group were incubated with 5μM Fluo-4 AM (Invitrogen, F14201) for 1 hour in KRBH solution, supplemented with 6 mM glucose and 0.1% BSA, at 37℃ in the dark. The islets were then transferred to a buffer solution containing 20mM glucose and incubated at 37℃ in the dark for 30 minutes before being plated in an imaging chamber for confocal microscopy on a Leica SP8 system. Time series images were acquired every 10 s (XYZT imaging, stack of 10 confocal images). Alpha cells were identified by their response to stimulation with 10 μM adrenaline. To visualize intracellular Ca^{2+} fluctuations, the average Fluo-4 AM fluorescence intensity per frame was measured using Leica Application Suite X (V2.0.1). Fluorescence intensity was displayed as the ratio of the original fluorescence intensity (F) to the initial

fluorescence intensity value (F0) (F/F0). The baseline (F0) of each group was defined as the average fluorescence intensity before stimulation with 1mM glucose.

2.8 DOTA-JR11 injection and tail-tip blood sampling

DOTA-JR11 was freshly prepared in sterile saline under light-protected conditions and administered *via* intraperitoneal injection (100 μL, 10 mg/kg) to five 18-week-old non-diabetic female NOD mice. Another five age- and cage-matched non-diabetic female NOD mice received an equal volume of sterile saline. Three hours post-injection, all mice were fasted. Starting from the time of intraperitoneal injection, tail-tip blood samples were collected every 6 hours thereafter. Blood volume collected at each time point did not exceed 30 μL. Part of the blood was immediately used for glucose measurement, while the remaining serum was collected and stored at –80°C for subsequent glucagon analysis.

2.9 Single cell sequencing data analysis

We utilized published single-cell sequencing data from GSE117770 (20), which reported single-cell sequencing of 8-, 14-, and 16-week-old non-diabetic NOD mice. The detail information about the single-cell sequencing, including sequencing platform, read depth, cell numbers per sample, mouse strain (pure NOD), and original data processing pipelines are described in the original publication (20). We re-analyzed these single-cell sequencing data, the quality filtering was performed using multiple filtering criteria including excluding cells with 25% of mitochondrial gene expression, cells fewer than 200 genes expressed, or cells with more than 8000 genes expressed. Remaining cells were normalized using the NormalizeData function with the LogNormalize method, and highly variable genes were identified using

FindVariableFeatures. Unsupervised analysis was carried out using principal component analysis (PCA) via the RunPCA function to identify principal components.The top principal components (PCs) were used for cell clustering. Cells with similar transcriptome profiles were clustered into 26 cell clusters corresponding to 10 cell types, including beta cells, alpha cells, delta cells, PP cells, acinar cells, endothelial cells, immune cells, fibroblasts, smooth-muscle cells, and erythroid-like cells. These cells were used for subsequent analysis. Pseudo-time analysis was performed using the Monocle2 package (21).

2.10 Algorithm for pancreatic islet clustering based on size, infiltration and endocrine cell proportion

All pancreatic islets were sequentially numbered and labeled with information on their origin (mouse ID), age, health status at the time of death, islet size, number of infiltrating immune cells, and proportion of three types of endocrine cells. Normalization was performed using the NormalizeData function, and feature variables were identified through FindVariableFeatures. Principal components were determined using RunPCA, and clustering was based on these results. The top principal components were used as input for Uniform Manifold Approximation and Projection (UMAP) analysis to determine the overall relationship between islets.

2.11 Statistical analysis

Raw data were analyzed with GraphPad Prism 9 software (GraphPad Software, La Jolla, CA, USA; RRID: SCR_002798). Data are presented as means ± SEM. No outlying values were excluded from the datasets used for statistical analysis. Two-way ANOVA followed by Bonferroni post hoc tests was used for two-factor assays. For

single-factor assays, unpaired t-tests or one-way ANOVA were employed. All data were first subjected to the Shapiro-Wilk normality test. If the data followed a Gaussian distribution, parametric tests were performed, followed by Bonferroni post hoc tests for three or more groups. If the data did not follow a Gaussian distribution, non-parametric tests (Mann-Whitney test for two groups or Kruskal-Wallis test with Dunn's post hoc test for three or more groups) were performed. Differences were considered to be statistically significant when $p < 0.05$.

3. Results

3.1 Dynamic analysis of endocrine cells reveals an increase of delta cells in non-diabetic NOD mice

We examined the pancreas of non-diabetic female NOD mice across six age groups: 5-9 weeks, 10-14 weeks, 15-19 weeks, 20-24 weeks, 25-30 weeks and >30 (31-32) weeks. Immunofluorescence analysis was carried out on islets from 66 individual female non-diabetic NOD mice at different ages to quantify the number and proportion of alpha, beta and delta cells, as well as immune cells (Fig. 1A). As shown in Fig. 1B-1C, following immune cell infiltration, islets became smaller (Fig. 1B), and immune cells exhibited a trend toward increase and then decrease (although not statistically significant, Fig. 1C). The beta cell area and ratio relative to all endocrine cells were significantly higher in 5-9-week-old mice compared to other age groups (Fig. 1D-1E). Therefore, we considered this age group (5-9 weeks) to be the baseline control with relatively little insulitis and used mice aged 10-14 weeks as having the main period of insulitis to which the other age groups were compared, when testing for statistical significance. The alpha cell area decreased upon insulitis

onset and remained relatively constant at later stages, while the alpha cell ratio related to all endocrine cells initially increased and then decreased (Fig. 1F-1G). Notably, from 10-14 weeks to 20-24 weeks, the delta cell area and ratio to all endocrine cells continued to increase after insulitis onset (Fig. 1H-1I).

3.2 A new classification of islet heterogeneity indicates an increase in somatostatin-positive islets

To further investigate changes in pancreatic islets at different ages of non-diabetic NOD mice, we analyzed islet heterogeneity in each age group, including islet size, endocrine cell proportions and degree of infiltration. As shown in Fig. 1J, islets from mice of different age groups exhibited significant heterogeneity in size, number of immune cells, and endocrine cell composition. Heterogeneity was also observed within groups of mice of the same age.

To further describe this heterogeneity systematically, we used an algorithm to analyze 486 islets from 66 non-diabetic NOD mice in order to determine their origin. We assessed four indicators for each islet: the number of infiltrating immune cells, the proportion of three endocrine cell types, dimensionality reduction, and clustering. This resulted in five distinct subtypes (Fig. 1K, Fig. S3A). As shown in Fig. 1L-1O and Fig. S3B, cluster 1 contained only beta cells and was defined as CD45+/-Ins+Gcg+Sst+/- type (including both CD45+ and CD45- subtypes); clusters 2 and 3 were heavily infiltrated by immune cells but differed in delta cell ratios, defined as CD45+Ins-Gcg+Sst+and CD45+Ins-Gcg+Sst- types, respectively; clusters 4 and 5, without immune infiltration, were defined as CD45-Ins-Gcg+Sst+ and CD45-Ins-Gcg+Sst- types, respectively. Statistical analysis revealed that the proportion of clusters with more delta cell-positive islets (clusters 2 and cluster 4, in

green) increased with age, while the proportion of clusters with fewer delta cells in the islets (clusters 3 and cluster 5, in blue) decreased (Fig. 1P). Combined with the earlier findings of increased delta-cell area and ratio (Fig. 1H and 1I), these data suggested that somatostatin-positive islets increased during autoimmunity progression in non-diabetic NOD mice.

3.3 Alpha cells transdifferentiate into delta cells in non-diabetic NOD mice

Given the observed increase in somatostatin-positive islets and delta cells in older non-diabetic mice (Fig. 1H and Fig. 1P), we hypothesized that there might be transdifferentiation from other endocrine cells to delta cells at different ages of non-diabetic NOD mice. Intriguingly, glucagon and somatostatin double-positive cells (alpha^{+}delta^{+} cells) significantly increased in non-diabetic mice after immune infiltration (> 10-14 weeks), peaking in 15-19-week-old mice. (Fig. 2A-2C). These data indicated ongoing either alpha-to-delta cell or delta-to-alpha cell conversion in some islets.

To investigate the potential direction of transdifferentiation, we re-analyzed a previously published single-cell RNA sequencing dataset (GEO accession: GSE117770) which included islets from 8-, 14-, and 16-week-old non-diabetic NOD mice (20). We reconstructed the dimensionality reduction based on tSNE (t-distributed stochastic neighbor embedding) and divided the cells into clusters (Fig. S4). We next isolated all alpha and delta cells from different ages for further analysis (Fig. 2D). Based on glucagon and somatostatin expression levels, we found more double-positive cells in 14- and 16-week-old mice (Fig. 2E), consistent with our immunostaining data. In addition, alpha cells from different ages were also analyzed for their identity (Fig. 2F). Notably, alpha cells from 14-week-old mice expressed

high levels of delta-cell marker genes, suggesting a subset of alpha cells may be undergoing transdifferentiation.

To verify our hypothesis and determine the direction of differentiation, we performed pseudo-time series analysis of alpha and delta cell clusters from GSE117770 (Fig. 2G) and constructed a trajectory (Fig. 2H and 2I). Our results showed that the trajectory comprised four branches and three decision points, dividing cells into seven states (Fig. 2J). Alpha cells were located near the left pole, while delta cells were near the right pole (Fig. 2H). Cells near the poles indicated mature states, whereas cells in the middle zone represented transitional states, which are relatively less well defined (Fig. 2H). As shown in Fig. 2J, states 3, 4, 5 and 6 corresponded to mature alpha cells, and states 1 and 7 to mature delta cells, while state 2 represented transitional cells. Interestingly, double positive cells were predominantly located in states 2 and 1, mainly from 14- and 16- week-old mice (Fig. 2K). These data indicated that transitional cells, which were double-positive, developed into delta cells, retaining glucagon. Collectively, our results suggested that a subset of alpha cells transdifferentiated into delta cells during diabetes development in NOD mice.

3.4 Alpha cell dedifferentiation followed by transdifferentiation into delta cells in non-diabetic NOD mice

Our foregoing data demonstrated that during insulitis development in non-diabetic NOD mice, some alpha cells became double hormone-positive cells before transforming into delta cells. To investigate whether this transdifferentiation occurred directly or involved dedifferentiation followed by transdifferentiation, we focused on neurog3 (Ngn3), a master transcription factor regulating endocrine cell differentiation and maturation, primarily expressed in endocrine precursor cells (22).

We performed immunofluorescent staining on islets from non-diabetic NOD mice to detect glucagon, somatostatin and Ngn3. As shown in Fig. 3A and 3B, many Ngn3-positive alpha cells were detected at 5-9 weeks, 10-14 weeks and 15-19 weeks, peaking at 10-14 weeks. Most Ngn3 positive cells were glucagon positive (Fig. 3A). Interestingly, the peak of Ngn3 positive cells (Fig. 3B solid line) slightly preceded the peak of glucagon and somatostatin double-positive cells (Fig. 3B dashed line).

To confirm that the alpha cells in non-diabetic mice dedifferentiated and then transdifferentiated into delta cells, we performed immunostaining with another precursor and dedifferentiation marker, Sox9. As shown in Fig. 3C, many glucagon positive cells at 13-30 weeks were Sox9 positive, peaking at 13 weeks. Additionally, dedifferentiation marker Aldh1a3 and precursor cell marker Nkx6.1 were also found in some alpha cells at 14 weeks (Fig. S5). We also analyzed these precursor and dedifferentiation genes using the published single-cell sequencing data GSE117770 (20). As shown in Fig. 3D, *Ngn3* levels in alpha cells gradually increased from 8 to 16 weeks during autoimmune diabetes progression. In addition, *Sox9* and *Aldh1a3* levels increased at 14 weeks, and *Nkx6.1* increased by 16 weeks, consistent with our immunostaining results.

Taken together, these data suggested that alpha cells firstly dedifferentiated and then transdifferentiated into delta cells during immune infiltration between 14-19 weeks.

3.5 Alpha cell proliferation occurs simultaneously with alpha cell dedifferentiation

Given that the alpha cell population did not decrease and remained relatively constant after 10-14 weeks of age (Fig. 1F), we then investigated whether alpha cells

proliferated during progression of autoimmunity in non-diabetic NOD mice. By immunostaining for the proliferation marker Ki67, we found that delta cell proliferation rates were maintained at a low level across most age groups of non-diabetic NOD mice, both in terms of area and ratio (Fig. 3E-3G). However, delta cell proliferation increased in late stage mice, particularly in non-diabetic mice older than 30 weeks (Fig. 3F-3G). In contrast, alpha cells exhibited high levels of proliferation during later insulitis (> 10-14 weeks), especially between 10 to 19 weeks (Fig. 3E-3G). The peak periods of alpha cell proliferation coincided with the presence of glucagon and somatostatin double-positive cells (Fig. 2A-2C), indicating that alpha cell proliferation occurred simultaneously with alpha cell dedifferentiation, maintaining the alpha cell mass relatively constant in non-diabetic NOD mice.

3.6 Increased delta cells suppress glucagon secretion in older non-diabetic mice

To investigate whether the increase in delta cells affected hormone secretion from endocrine cells, we isolated islets from non-diabetic NOD mice of different ages and measured glucagon, insulin and somatostatin content (Fig. 4A-4C). As expected, glucagon levels increased with age (Fig. 4A), while insulin content in islets gradually decreased (Fig. 4B), and somatostatin content gradually increased (Fig. 4C), consistent with changes in the beta and delta cells, respectively (Fig. 1D and 1H). Since somatostatin receptor 2 (Sstr2) is the primary somatostatin receptor expressed in human and mouse alpha cells (23), we then cultured islets from non-diabetic NOD mice of different ages *in vitro*, with or without the Sstr2 inhibitor DOTA-JR11, and measured hormone secretion levels after 2 hours (Fig. S6) and 24 hours (Fig. 4D-F) of culture. Interestingly, DOTA-JR11 treatment significantly increased the glucagon secretion (Fig. 4D and Fig. S6A), while there was no significant change in insulin

(Fig. 4E and Fig. S6B) or somatostatin (Fig. 4F and Fig. S6C) secretion upon Sstr2 inhibition, indicating the inhibitory effect of somatostatin on glucagon responses. Moreover, somatostatin secretion in islets from older mice also increased with age (Fig. 4F).

Since glucagon secretion depends on cytoplasmic Ca^{2+} concentration (24), we evaluated the Ca^{2+} response of alpha cells (identified by response to adrenaline stimulation) from non-diabetic NOD mice at different ages using the Ca^{2+} indicator Fluo-4 AM (25) and recorded these with confocal microscopy time-lapse imaging (Fig. S7). As shown in Fig. 4G, with age, the alpha cell response to low glucose gradually decreased (Fig. 4G, times between 200 to 400 s), including the response amplitude (Fig. 4H, 1 mM glucose) and response speed (Fig. 4I, 1 mM glucose). Additionally, alpha cells in older (20-30-week-old) mice exhibited dysfunctional responses to adrenaline (Fig. 4G, times between 400 to 600 s). Interestingly, after Sstr2 inhibitor treatment, the oscillation amplitude of cytoplasmic Ca^{2+} concentration in alpha cells significantly increased in older mice, while the response was weaker in younger mice (5-14 weeks old) (Fig. 4G, times between 600 to 800 s).

To investigate whether DOTA-JR11 treatment has a similar effect on glucagon secretion *in vivo*, we administrated 18-week-old non-diabetic female NOD mice with DOTA-JR11. We then fasted these mice stared from 3 hours after injection, then measured the glucose and glucagon levels at 6 h and 12 h after injection (Fig. 4J-4K). All mice showed a gradual decrease of glucose level and an increase of glucagon level at 6 h after injection, while the DOTA-JR11-injected group showed significantly higher glucagon level than control group. At the 12 h, the DOTA-JR11 injected mice show higher glucose and glucagon levels compared with control group. These data may indicate that blockade of somatostatin signaling reverses α-cell suppression in

non-diabetic NOD mice *in vivo*.

Taken together, these results indicate that the increase in delta cells, associated with age, suppresses glucagon secretion in non-diabetic NOD mice through somatostatin production.

3.7 Alpha-to-delta cell transdifferentiation was not observed in diabetic NOD mice

To explore whether alpha-to-delta cell transdifferentiation also occurred in diabetic NOD mice, we harvested pancreata from 61 NOD mice with varying ages of diabetes onset and performed immunostaining (Fig. S8A). There were no statistically significant differences in islet size or the number of infiltrating immune cells within different groups in diabetic mice, while the islet size and infiltrating immune cells were lower than non-diabetic groups (Fig. 5A-5B). Beta cell area and ratio were very low in all diabetic mice (Fig. 5C-5D), while alpha cell area and ratio remained unchanged (Fig. 5E-5F). Although delta cell numbers showed a trend to increase with age in diabetic NOD mice, this was not statistically significant due to variability (Fig. 5G-5H). Moreover, the delta cell numbers were also no difference compared with same age of non-diabetic NOD mice (Fig. 5G). Although the ratio of delta cell in earlier stages diabetic NOD mice is higher than non-diabetic group, it is most likely due to the extremely loss of beta cells (Fig. 5H).

The islets in diabetic mice were also highly heterogeneous (Fig. S8B). We classified the islets of diabetic mice according to the same clustering method used for non-diabetic mice (clusters 1 to 5 as shown in Fig. 1L-1O). Compared with the changes in the proportion of islet clusters in non-diabetic mice of different age groups (Fig. 1P), the proportions of the five clusters in diabetic mice at different ages of

diabetes development were similar (Fig. 5I).

We then stained and counted alpha+delta+ double-positive cells (Fig. S9A) and Ngn3-positive cells (Fig. S9B) in diabetic NOD mice of all ages. The numbers of alpha+delta+ double-positive cells were very low in diabetic mice (Fig. 5J-5K and Fig. S9A). Furthermore, Ngn3-positive and Sox9-positive alpha cells were barely detectable (Fig. 5L, Fig. S9B and Fig. S9C). Aldh1a3- or Nkx6.1-positive alpha cells were also scarcely detected in 14-week-old diabetic NOD mice (Fig. S10A-S10B). In addition, the proliferation of alpha and delta cells in diabetic mice was much lower compared to non-diabetic mice (Fig. 5M-5N and Fig. S11). Taken together, these data suggest that alpha-to-delta cell transdifferentiation was not observed in diabetic NOD mice.

4. Discussion

The non-obese diabetic (NOD) mouse, is widely used as an T1D animal model. Although they share the same genetic background, approximately 20% of female NOD mice do not develop diabetes. Understanding why these mice do not process to diabetes during the autoimmunity progression remains a subject of significant scientific interest. Studies have revealed that sex hormones, genetic heterogeneity, gut microbiome, regulatory T cells, environmental factors are associated with the prevention of diabetes in NOD mice (26-28). Moreover, the non-diabetic NOD mice exhibit distinct islet characteristics compared to diabetic mice (16). However, the specific mechanisms underlying changes in pancreatic islet endocrine cells remain unclear.

In this study, we examined the composition of alpha, beta and delta cells in islets

459 at multiple time points throughout the progression of autoimmunity in the
460 non-diabetic NOD mice. We observed that the alpha-cell area remained relatively
461 constant after immune cell infiltration (Fig. 1F), while the delta cell area significantly
462 increased in older mice (Fig. 1H). There was notable heterogeneity in islet size,
463 endocrine cell composition and degree of infiltration (Fig. 1J). Although it is known
464 that there is heterogeneity in beta-cell destruction and immune cell infiltration (16,
465 29), our study provides a more comprehensive evaluation of islet heterogeneity,
466 including size, composition of different endocrine cells, and immune infiltration at
467 different ages during autoimmunity progression. Based on these observations, we
468 proposed a new classification system, dividing islets into five subtypes (Fig. 1K-1O),
469 based on the beta cell composition, immune cell infiltration, and further subdivisions
470 according to alpha and delta cell composition, providing a more detailed description
471 than previously published (30, 31). Using this new classification, we found an
472 increase in somatostatin-positive islets following immune cell infiltration (Fig. 1P).

473 In 10-14- and 15-19-week-old (established insulitis and pre-diabetes)
474 non-diabetic NOD mice, we observed a significant increase in glucagon and
475 somatostatin double-positive cells (Fig. 2A-2C). Furthermore, we demonstrated that
476 these double-positive cells were undergoing transdifferentiation from alpha to delta
477 cells (Fig. 2D-2K). These alpha-to-delta transdifferentiated cells first dedifferentiated
478 into precursor cells before differentiating further into delta cells, as evidenced by
479 increased expression of Ngn3, Sox9, Aldh1a3 and Nkx6.1 (Fig. 3A-D), accompanied
480 by simultaneous alpha cell proliferation (Fig. 3E-G). The alpha cell to delta cell
481 transdifferentiation in non-diabetic NOD mice was not due to beta-cell loss, since the
482 beta-cell keep constant after 15-19 weeks old in non-diabetic mice (Fig. 1D and Fig.
483 5D) and the replication of delta cells is pretty low at these stages (except >30 weeks

old NOD mice) (Fig. 3G). The dedifferentiation of alpha cell may associate with the inflammatory cytokines (IL-1β, IFN-γ, TNF-α). Indeed, we compared the gene profiles of glucagon and somatostatin double positive cell to the glucagon or somatostatin alone positive cell using published single-cell RNA-seq (GSE117770), and identified IFN-γ pathway specifically increased in the glucagon and somatostatin double positive clusters (Fig. S12A-12E). Moreover, GESA (gene set enrichment analysis) also indicated that downstream signaling cascade of IFN-γ, the JAK-STAT pathway was significantly enriched in double positive cells (Fig. S12F). Experimentally, we then treated αTC1-6 cells with IFN-γ. Interestingly, IFN-γ incubation significantly increased the dedifferentiation-associated genes Aldh1a3, and reduced the level of glucagon protein (Fig. S12G-12I). These data suggested that IFN-γ may serve as potential triggers for induction of α cell dedifferentiation.

However, although we observed a trend toward increased delta cells in diabetic NOD mice, we did not detect alpha-to-delta cell transdifferentiation in these mice (Fig. 5). We speculated that alpha-to-delta transdifferentiation in diabetic mice may occur before the diabetes onset based on several evidences. Firstly, the occurrence of alpha cells to delta cells transdifferentiation was in the stages between 10-14 and 15-19-week old non-diabetic mice (Fig. 2A-2C, Fig. 3A-3B), while the delta cell mass of these stages was slightly lower than diabetic groups, albeit there was no significant difference in delta cell mass between diabetic and non-diabetic mice (Fig. 5G). Secondly, the delta cell mass also kept increasing along with age at the point of they developed diabetes (Fig. 5G). Thirdly, we did not detect the delta-cell proliferation in the diabetic mice, suggesting that the increased δ cell mass was not due to delta-cell proliferation (Fig. 5M-5N). The last but not the least, the non-diabetic mice we harvested earlier stages may develop to diabetes in the later stage. Taken together,

based on these evidences, we propose that the increased delta cell mass in diabetic mice is a result of transdifferentiation occurred before the diabetes onset, before the stage of we harvested them. Nevertheless, the possibility that alpha-to-delta cell transdifferentiation occurs before diabetes onset cannot be excluded based on our current data. Somatostatin secreted by delta cells significantly inhibits glucagon secretion by alpha cells (32). Studies also suggested that delta cells are increased in individuals with T1D and diabetic NOD mice, exhibiting greater activation in people with T1D, a which may play a protective role against hyperglycemia (33-35). Conversely, Sstr2 antagonism ameliorates insulin-induced hypoglycemia by enhancing glucagon responses (36). Our data indicate that increased delta cells and somatostatin in pancreatic islets significantly inhibit alpha cell function during autoimmunity progression in non-diabetic mice (Fig. 4). Delta cells increase as beta cells are lost, and somatostatin from these cells inhibits glucagon secretion, potentially protecting against hyperglycemia and delaying diabetes onset in NOD mice. However, increased inhibition of glucagon secretion may also lead to alpha cell dysfunction in response to low glucose.

We propose a new working model for changes within pancreatic islets during progression of autoimmunity in non-diabetic NOD mice (Fig. 6). During autoimmunity progression, immune cells infiltrate the islets, leading to a gradual of beta cell loss. Islets then undergo two distinct transition paths. In some islets, the few initial delta cells are lost along with beta cells, resulting in islets predominantly composed of alpha cells. These islets increase rapidly in younger non-diabetic mice but decrease in older mice, suggesting that this subtype gradually shrinks and eventually disappears *in vivo*. In contrast, another type of islet becomes more abundant in older non-diabetic mice, characterized by a significant increase in delta

cell numbers as beta cells decline, and this type of islet can survive longer. This change is not age-dependent, as no significant differences in islet type proportions were observed across various age groups in diabetic mice. While the triggers for this process remain unclear, our data suggest that the increase in delta cells is predominantly due to transdifferentiation from alpha cells, which firstly undergo dedifferentiation and then eventually transdifferentiate into delta cells. The increased delta cell areas in the islets contribute to higher somatostatin secretion, which inhibits glucagon release from adjacent alpha cells and mitigates hepatic glucose production, which may associate with lower glucose level in the non-diabetic NOD mice with higher delta cell mass, and may have a protective role in the prevention of onset of diabetes in NOD mice.

Overall, we investigated islet heterogeneity and hormone secretion during the progression of autoimmunity in non-diabetic NOD mice. We found that not only do endocrine cell numbers and functions change, but the cell composition within islets also undergoes transformation. These results enhance our understanding of the active roles played by alpha and delta cells in T1D pathophysiology and mechanisms that counteract hyperglycemia with the loss of insulin-producing beta cells. If this mechanism also occurs in humans, changes in the balance of alpha cells and delta cells may explain reduced hypoglycemic responses due to impaired glucagon counter-regulation in patients receiving exogenous insulin. However, the detailed mechanism of alpha cell to delta cell transdifferentiation requires further investigation, particularly its occurrence in humans. So far, none studies reported the detection of glucagon and somatostatin double-positive cells in the human T1D patients. However, studies have reported that the delta cell mass increased in human T1D patients (10). Our observation in NOD mice is consistent with human data, we only detect alpha to

559 delta cell transdifferentiation in non-diabetic NOD mice, but not in diabetic NOD
560 mice. Nevertheless, the alpha-to-delta cell transdifferentiation may occurs before
561 diabetes onset in human T1D patients.

562 Therapeutic approaches for T1D mostly rely on insulin treatment, which may
563 cause severe hypoglycemia due to alpha-cell defects and lack of glucagon response in
564 a subset of patients, a phenomenon recognized for many years (37). Effective
565 management of T1D should include a focus on glucagon secretion to prevent severe
566 hypoglycemia. Understanding the mechanisms underlying decreased glucagon
567 secretion during T1D pathogenesis is crucial. Glucagon secretion is regulated both
568 intrinsically (within the alpha cell itself) and in a paracrine manner (mediated by
569 factors released by beta and/or delta cells) (38). Hence, comprehending dynamic
570 compositional alteration of alpha, beta and delta cells in islets during human T1D,
571 could potentially provide new therapeutic avenues.

572

573

574 **Data availability**: The data generated in this study are available from the
575 corresponding authors on reasonable request.

576

577 **Supplemental material**: Supplemental Figs. S1–S12:
578 https://doi.org/10.6084/m9.figshare.29959619

579

580 **Acknowledgements:** We express our gratitude to Joanne Davies (Cardiff University)
581 for her invaluable advice and assistance concerning the maintenance and training in
582 NOD mouse colony management, and to Joanne Boldison (Exeter University) for her
583 expert advice on NOD islet cell analysis. We also acknowledge the members of the Li

laboratory for their constructive discussions. Additionally, we extend our thanks to Zhen Li, Yihong Wu, Lijuan Wang, and Yanhong Zou for their technical support.

Grants: This work was supported by grants from the Foreign Cooperation Project of Science and Technology, Fujian Province, China (2023I0002 to ML), Joint Funds for the innovation of science and Technology, Fujian province (2023Y9270), Natural Science Foundation of Xiamen, China (3502Z20227162 to M.L.), Xiang An Biomedicine Laboratory (2023XAKJ0102039 to M.L.) and the grants from Key Laboratory of Tropical Marine Ecosystem and Bioresource, Ministry of Natural Resources (2021ZD01 to ML).

Author contributions: M.L. is the guarantor of this work and, as such, had full access to all of the data in the study and takes responsibility for the integrity of the data and the accuracy of the data analysis. M.L. and F.S.W designed the study. Z.L., X.W., M.L., Q.K. and Q.R. performed key experiments. M.L., F.S.W., Z.L., Q.K., Y.Z. and Y.Z. participated in the planning of the work and the interpretation of the results. Z.L., drafted the manuscript. M.L., F.S.W., Q.J., revised the paper. All authors are in agreement with the final version of the manuscript.

Disclosures:

The authors declare that they have no conflicts of interest with the contents of this article.

References:

1. **Boldison J, and Wong FS**. Immune and Pancreatic beta Cell Interactions in Type 1 Diabetes. *Trends Endocrinol Metab* 27: 856-867, 2016.

2. **Brown RJ, Sinaii N, and Rother KI**. Too much glucagon, too little insulin: time course of pancreatic islet dysfunction in new-onset type 1 diabetes. *Diabetes Care* 31: 1403-1404, 2008.

3. **Sherr J, Tsalikian E, Fox L, Buckingham B, Weinzimer S, Tamborlane WV, White NH, Arbelaez AM, Kollman C, Ruedy KJ, Cheng P, Beck RW, and Diabetes Research in Children N**. Evolution of abnormal plasma glucagon responses to mixed-meal feedings in youth with type 1 diabetes during the first 2 years after diagnosis. *Diabetes Care* 37: 1741-1744, 2014.

4. **Raskin P, and Unger RH**. Effect of insulin therapy on the profiles of plasma immunoreactive glucagon in juvenile-type and adult-type diabetics. *Diabetes* 27: 411-419, 1978.

5. **Panzer JK, and Caicedo A**. Targeting the Pancreatic alpha-Cell to Prevent Hypoglycemia in Type 1 Diabetes. *Diabetes* 70: 2721-2732, 2021.

6. **Pechhold K, Zhu X, Harrison VS, Lee J, Chakrabarty S, Koczwara K, Gavrilova O, and Harlan DM**. Dynamic changes in pancreatic endocrine cell abundance, distribution, and function in antigen-induced and spontaneous autoimmune diabetes. *Diabetes* 58: 1175-1184, 2009.

7. **Plesner A, Ten Holder JT, and Verchere CB**. Islet remodeling in female mice with spontaneous autoimmune and streptozotocin-induced diabetes. *PLoS One* 9: e102843, 2014.

8. **Novikova L, Smirnova IV, Rawal S, Dotson AL, Benedict SH, and Stehno-Bittel L**. Variations in rodent models of type 1 diabetes: islet morphology. *J Diabetes Res* 2013: 965832, 2013.

9. **Kornete M, Beauchemin H, Polychronakos C, and Piccirillo CA**. Pancreatic islet cell phenotype and endocrine function throughout diabetes development in non-obese diabetic mice. *Autoimmunity* 46: 259-268, 2013.

10. **Jeffery N, Richardson S, Chambers D, Morgan NG, and Harries LW**. Cellular stressors may alter islet hormone cell proportions by moderation of alternative splicing patterns. *Hum Mol Genet* 28: 2763-2774, 2019.

11. **Zyznar ES, Pietri AO, Harris V, and Unger RH**. Evidence for the hormonal status of somatostatin in man. *Diabetes* 30: 883-886, 1981.

12. **Hill TG, Gao R, Benrick A, Kothegala L, Rorsman N, Santos C, Acreman S, Briant LJ, Dou H, Gandasi NR, Guida C, Haythorne E, Wallace M, Knudsen JG, Miranda C, Tolo J, Clark A, Davison L, Storling J, Tarasov A, Ashcroft FM, Rorsman P, and Zhang**

Q. Loss of electrical beta-cell to delta-cell coupling underlies impaired hypoglycaemia-induced glucagon secretion in type-1 diabetes. *Nat Metab* 6: 2070-2081, 2024.

13. **Pearson JA, Wong FS, and Wen L**. The importance of the Non Obese Diabetic (NOD) mouse model in autoimmune diabetes. *J Autoimmun* 66: 76-88, 2016.

14. **Atkinson MA, and Leiter EH**. The NOD mouse model of type 1 diabetes: as good as it gets? *Nat Med* 5: 601-604, 1999.

15. **Ferris ST, Carrero JA, and Unanue ER**. Antigen presentation events during the initiation of autoimmune diabetes in the NOD mouse. *J Autoimmun* 71: 19-25, 2016.

16. **Boldison J, Thayer TC, Davies J, and Wong FS**. Natural Protection From Type 1 Diabetes in NOD Mice Is Characterized by a Unique Pancreatic Islet Phenotype. *Diabetes* 70: 955-965, 2021.

17. **Kang Q, Jia J, Dean ED, Yuan H, Dai C, Li Z, Jiang F, Zhang XK, Powers AC, Chen W, and Li M**. ErbB3 is required for hyperaminoacidemia-induced pancreatic alpha cell hyperplasia. *J Biol Chem* 300: 107499, 2024.

18. **Yuan H, Kang Q, Li Z, Bai X, Jia J, Han D, Wu X, and Li M**. Crispr-Cas9 mediated complete deletion of glucagon receptor in mice display hyperglucagonemia and alpha-cell hyperplasia. *Biochem Biophys Res Commun* 643: 121-128, 2023.

19. **Jia J, Bai X, Kang Q, Jiang F, Wong FS, Jin Q, and Li M**. Blockade of glucagon receptor induces alpha-cell hypersecretion by hyperaminoacidemia in mice. *Nat Commun* 16: 2473, 2025.

20. **Thompson PJ, Shah A, Ntranos V, Van Gool F, Atkinson M, and Bhushan A**. Targeted Elimination of Senescent Beta Cells Prevents Type 1 Diabetes. *Cell Metab* 29: 1045-1060 e1010, 2019.

21. **Trapnell C, Cacchiarelli D, Grimsby J, Pokharel P, Li S, Morse M, Lennon NJ, Livak KJ, Mikkelsen TS, and Rinn JL**. The dynamics and regulators of cell fate decisions are revealed by pseudotemporal ordering of single cells. *Nat Biotechnol* 32: 381-386, 2014.

22. **Rukstalis JM, and Habener JF**. Neurogenin3: a master regulator of pancreatic islet differentiation and regeneration. *Islets* 1: 177-184, 2009.

23. **Blodgett DM, Nowosielska A, Afik S, Pechhold S, Cura AJ, Kennedy NJ, Kim S, Kucukural A, Davis RJ, Kent SC, Greiner DL, Garber MG, Harlan DM, and diIorio P**. Novel Observations From Next-Generation RNA Sequencing of Highly Purified Human Adult and Fetal Islet Cell Subsets. *Diabetes* 64: 3172-3181, 2015.

24. **Tengholm A, and Gylfe E**. cAMP signalling in insulin and glucagon secretion. *Diabetes Obes Metab* 19 Suppl 1: 42-53, 2017.

25. **Liew LC, Poh BM, An O, Ho BX, Lim CYY, Pang JKS, Beh LY, Yang HH, and Soh BS**. JAK2 as a surface marker for enrichment of human pluripotent stem cells-derived ventricular cardiomyocytes. *Stem Cell Res Ther* 14: 367, 2023.

26. **Marino E, Richards JL, McLeod KH, Stanley D, Yap YA, Knight J, McKenzie C, Kranich J, Oliveira AC, Rossello FJ, Krishnamurthy B, Nefzger CM, Macia L, Thorburn A, Baxter AG, Morahan G, Wong LH, Polo JM, Moore RJ, Lockett TJ, Clarke JM, Topping DL, Harrison LC, and Mackay CR**. Gut microbial metabolites limit the frequency of autoimmune T cells and protect against type 1 diabetes. *Nat Immunol* 18: 552-562, 2017.

27. **Wen L, Ley RE, Volchkov PY, Stranges PB, Avanesyan L, Stonebraker AC, Hu C, Wong FS, Szot GL, Bluestone JA, Gordon JI, and Chervonsky AV**. Innate immunity and intestinal microbiota in the development of Type 1 diabetes. *Nature* 455: 1109-1113, 2008.

28. **Lee J, Yurkovetskiy LA, Reiman D, Frommer L, Strong Z, Chang A, Kahaly GJ, Khan AA, and Chervonsky AV**. Androgens contribute to sex bias of autoimmunity in mice by T cell-intrinsic regulation of Ptpn22 phosphatase expression. *Nat Commun* 15: 7688, 2024.

29. **Ilonen J, Lempainen J, and Veijola R**. The heterogeneous pathogenesis of type 1 diabetes mellitus. *Nat Rev Endocrinol* 15: 635-650, 2019.

30. **Catrina AM, Popa MA, Văcaru AM, and Fenyo IM**. Inflammatory status of the pancreas in NOD mice that do not develop overt diabetes. *Rom J Morphol Embryol* 62: 109-115, 2021.

31. **Benkahla MA, Sabouri S, Kiosses WB, Rajendran S, Quesada-Masachs E, and von Herrath MG**. HLA class I hyper-expression unmasks beta cells but not alpha cells to the immune system in pre-diabetes. *J Autoimmun* 119: 102628, 2021.

32. **Gao R, Yang T, and Zhang Q**. δ-Cells: The Neighborhood Watch in the Islet Community. *Biology (Basel)* 10: 2021.

33. **Miranda C, Begum M, Vergari E, and Briant LJB**. Gap junction coupling and islet delta-cell function in health and disease. *Peptides* 147: 170704, 2022.

34. **Piran R, Lee SH, Li CR, Charbono A, Bradley LM, and Levine F**. Pharmacological induction of pancreatic islet cell transdifferentiation: relevance to type I diabetes. *Cell Death Dis* 5: e1357, 2014.

35. **Reddy S, Chai RC, Rodrigues JA, Hsu TH, and Robinson E**. Presence of residual beta cells and co-existing islet autoimmunity in the NOD mouse during longstanding diabetes: a combined histochemical and immunohistochemical study. *J Mol Histol* 39: 25-36, 2008.

36. **Yue JT, Riddell MC, Burdett E, Coy DH, Efendic S, and Vranic M**. Amelioration of

713 hypoglycemia via somatostatin receptor type 2 antagonism in recurrently hypoglycemic
714 diabetic rats. *Diabetes* 62: 2215-2222, 2013.

715 37. **Gerich JE, Langlois M, Noacco C, Karam JH, and Forsham PH**. Lack of glucagon
716 response to hypoglycemia in diabetes: evidence for an intrinsic pancreatic alpha cell defect.
717 *Science* 182: 171-173, 1973.

718 38. **Walker JN, Ramracheya R, Zhang Q, Johnson PR, Braun M, and Rorsman P**.
719 Regulation of glucagon secretion by glucose: paracrine, intrinsic or both? *Diabetes Obes*
720 *Metab* 13 Suppl 1: 95-105, 2011.
721

722

Figures and legends.

Figure 1. Dynamic changes and high heterogeneity in endocrine cell proportions across different ages of non-diabetic NOD mice.

(**A**) Representative images of endocrine cells in non-diabetic NOD mice from various age groups. The upper labels indicate the respective age groups. DAPI-stained nuclei (blue), glucagon-stained alpha cells (green), insulin-stained beta cells (red), somatostatin-stained delta cells (magenta), and CD45-stained immune cells (white) are shown. (**B-C**) Comparison of islet size (B) and immune cell area (C) across different ages. Sample sizes (mice/islets per group) were as follows: 5-9 weeks (10/105), 10-14 weeks (11/90), 15-19 weeks (11/78), 20-24 weeks (11/85), 25-30 weeks (11/63), and >30 weeks (12/65). (**D-I**) Mean areas and proportions of beta, alpha, and delta cells relative to total endocrine cells in non-diabetic mice in the same age groups as in B-C, using the same sample sizes per group. (**J**) Analysis of islet heterogeneity in terms of composition and quantity of alpha, beta, and delta cells at different ages, based on 66 non-diabetic NOD mice and 486 islets. The x-axis shows the age of the mice, while the y-axis represents the square of the immune cell area surrounding the islets. The bubbles indicate islet area, with colors representing green for alpha cells, orange for beta cells, and blue for delta cells. (**K**) Uniform Manifold Approximation and Projection (UMAP) clustering of the same 486 islets, grouped into five islet types (cluster 1-5). Number of mice/islets per cluster: cluster 1 (87/272), cluster 2 (93/224), cluster 3 (67/123), cluster 4 (54/121), and cluster 5 (34/58). (**L-O**) Violin plots showing the ratio of areas occupied by immune cells (L), beta cells (M), alpha cells (N), and delta cells (O) relative to the total islet area in different clusters. The colors of the clusters in the violin plots are indicated on the right. (**P**) Proportion

748 of the five types of islets at different ages of non-diabetic mice.. Data are presented as
749 mean ± SEM, with significance determined by one-way ANOVA compared to the
750 10-14-week age group, which represents the main period of insulitis in pre-diabetes:
751 *$P < 0.05$, **$P < 0.01$, and ****$P < 0.0001$.
752
753
754 **Figure 2. Alpha cells transdifferentiate into delta cells in non-diabetic NOD mice.**
755 (**A**) Representative images of glucagon and somatostatin double-positive endocrine
756 cells in non-diabetic NOD mice at different ages, as indicated by the upper labels. The
757 cells within the dashed boxes are magnified in the right panel of each image. Yellow
758 arrows indicate glucagon and somatostatin double-positive cells. DAPI-stained nuclei
759 (blue), glucagon-stained alpha cells (green), insulin-stained beta cells (red), and
760 somatostatin-stained delta cells (magenta) are shown. (**B**-**C**) Quantification of the area
761 (B) and proportion (C) of alpha+delta double-positive cells relative to all endocrine
762 cells at different ages. Sample sizes (mice/islets per group) were as follows: 5-9
763 weeks (10/105), 10-14 weeks (11/90), 15-19 weeks (11/78), 20-24 weeks (11/85),
764 25-30 weeks (11/63), and >30 weeks (12/65). (**D**) t-SNE projection based on marker
765 genes of alpha and delta cells, and NOD mouse sources from different age groups for
766 subsequent analysis (Based on GSE117770). (**E**) t-SNE projection of alpha and delta
767 cells based on glucagon (*gcg*) and somatostatin (*sst*) expression levels. Scale ranges
768 correspond to double gene (*gcg* and *sst*) expression as indicated. The red dashed line
769 highlights cells with high expression of both *gcg* and *sst*. (**F**) Expression levels of
770 endocrine cell markers in isolated alpha cells from different ages. Selected endocrine
771 cell genes are indicated on the left. Scale ranges correspond to gene expression levels
772 as indicated. (**G-I**) Pseudotime trajectory analysis of alpha and delta cells from

different ages based on pseudotime values (G), cell types (H), and ages (I). Numbers 1, 2, and 3 indicate decision points 1, 2, and 3, respectively. In panel E, color gradation depends on the pseudotime value ranging from 0 to 30. (**J**) Total alpha and delta cells from different ages were divided into seven clusters based on pseudotime trajectory analysis. The proportion of cells from each age group in each cluster is shown in the pie charts. (**K**) Expression of glucagon-somatostatin (*gcg-sst*) double-positive cells along the pseudotime trajectory. Color indicates the expression level in each cell. Data are presented as mean ± SEM, with significance determined by one-way ANOVA: $^{**}P < 0.01$, $^{****}P < 0.0001$.

Figure 3. Analysis of alpha cell dedifferentiation and proliferation in non-diabetic NOD mice at different ages.

(**A**) Representative images of endocrine cells in non-diabetic NOD mice at different ages, as indicated by the upper labels. The dashed box is magnified in the right panels of each image. Yellow arrows indicate Ngn3-positive cells. DAPI-stained nuclei (blue), glucagon-stained alpha cells (green), somatostatin-stained delta cells (magenta), and Ngn3-positive cells are stained in red. (**B**) Quantification of Ngn3-positive area at different ages in NOD mice. The blue solid line indicates the area of alpha+ Ngn3+ double-positive cells. Sample sizes (mice/islets per group) were as follows: 5-9 weeks (3/21), 10-14 weeks (3/17), 15-19 weeks (3/16), 20-24 weeks (3/15), 25-30 weeks (3/14), and >30 weeks (3/15). The magenta dashed line indicates the area of alpha+ delta+ double-positive cells. Sample sizes (mice/islets per group) were as follows: 5-9 weeks (10/105), 10-14 weeks (11/90), 15-19 weeks (11/78), 20-24 weeks (11/85), 25-30 weeks (11/63), and >30 weeks (12/65). (**C**)

Representative images of endocrine cells in non-diabetic NOD mice at different ages, as indicated by the upper labels. The dashed box is magnified in the right panels of each image. Yellow arrows indicate Sox9-positive cells. DAPI-stained nuclei (blue), glucagon-stained alpha cells (green), somatostatin-stained delta cells (magenta), and Sox9-positive cells are stained in red. (**D**) Expression levels of several marker genes in alpha cells from mice of different ages based on single-cell sequencing data (GSE117770). Scale ranges correspond to gene expression levels as indicated. (**E**) Representative images of Ki67-positive alpha and delta cells in non-diabetic NOD mice at different ages, as indicated by the upper labels. The dashed box is magnified in the side panels of each image. DAPI-stained nuclei (blue), glucagon-stained alpha cells (green), somatostatin-stained delta cells (white), and Ki67-positive cells are stained in red. (**F**-**G**) Quantification of Ki67-positive alpha and delta cell area (F) and proportion (G) at different ages. Sample sizes (mice/islets per group) were as follows: 5-9 weeks (4/44), 10-14 weeks (4/42), 15-19 weeks (4/46), 20-24 weeks (4/41), 25-30 weeks (5/40), and >30 weeks (5/43). Data are presented as mean ± SEM, with significance determined by one-way ANOVA compared to the 5-9-week age group: $^{**}P < 0.01$, $^{***}P < 0.001$, $^{****}P < 0.0001$.

Figure 4. The increased delta cells suppress alpha cell glucagon secretion by paracrine inhibition.

(**A**-**C**) The content of glucagon (A), insulin (B), and somatostatin (C) in islets from non-diabetic NOD mice at different ages. Data are presented for n = 10 islets from n = 3 mice per age group. (**D**-**F**) Secretion of glucagon (D), insulin (E), and somatostatin (F) with and without DOTA-JR11 after culturing islets from non-diabetic NOD mice

at different ages for 24 hours in vitro. Data are presented for n = 5 islets from n = 3 mice. The numbers above the bars in panel D indicate the fold changes in glucagon secretion upon DOTA-JR11 treatment of islets from mice of the same age. (**G**) Time course of average Ca^{2+} oscillations in alpha cells in response to a series of stimulations. The calcium influx response for each alpha cell was normalized to the initial fluorescence intensity (5.5 mM glucose). Sample sizes (mice/alpha cells per group) were as follows: 5-9 weeks (3/52), 10-14 weeks (3/47), 15-19 weeks (3/36), 20-24 weeks (3/41), and 25-30 weeks (3/33). (**H**) Area under the curve (AUC) of alpha cell responses to different stimuli from mice of different ages. (**I**) Time to reach peak intensity of alpha cell responses to different stimuli from mice of different ages. (J-K) Serial tail-tip blood sampling to monitor blood glucose (J) and plasma glucagon levels (K) in mice after SSTR2 inhibitor (DOTA-JR11) injection. 18 weeks old non-diabetic NOD female mice were used, and mice started to fast from 3 hours after injection. Data represent mean ± SEM. Statistical significance was determined by one-way ANOVA (A-C), Student's t-test and two-way ANOVA (D-F), and one-way ANOVA (H-I): $*P < 0.05$, $**P < 0.01$, $***P < 0.001$, $****P < 0.0001$.

Figure 5. Alpha to delta cell transdifferentiation was not observed in diabetic NOD mice.

(**A-B**) Comparison of islet size (A) and immune cell area (B) in diabetic NOD mice with non-diabetic mice at different ages. Sample sizes (mice/islets per group) were as follows: 10-14 weeks (10/60), 15-19 weeks (13/65), 20-24 weeks (14/62), 25-30 weeks (12/62), and >30 weeks (12/63). (**C-H**) Quantification of beta, alpha, and delta cell areas and their proportions in diabetic NOD mice, and compared with

non-diabetic mice Sample sizes per group was same as A-B. (**I**) Proportion of the five types of islets at different ages in diabetic NOD mice, classified based on Fig. 2D. (**J-K**) Quantification of alpha+ delta+ double-positive cell areas (J) and ratios (K) in NOD mice that developed diabetes at different ages, and compared with non-diabetic mice. Sample sizes (mice/islets per group) were as follows: 10-14 weeks (10/60), 15-19 weeks (13/65), 20-24 weeks (14/62), 25-30 weeks (12/62), and >30 weeks (12/63). (**L**) Quantification of Ngn3-positive area in NOD mice that developed diabetes at different ages, and compared with non-diabetic mice. Sample sizes (mice/islets per group) were as follows: 10-14 weeks (3/12), 15-19 weeks (3/13), 20-24 weeks (3/13), 25-30 weeks (3/11), and >30 weeks (3/10). (**M-N**) Quantification of Ki67-positive alpha and delta cell areas (M) and ratios (N) in NOD mice that became diabetic at different ages. Sample sizes (mice/islets per group) were as follows: 10-14 weeks (4/35), 15-19 weeks (4/30), 20-24 weeks (5/35), 25-30 weeks (4/33), and >30 weeks (5/32). Data are presented as mean ± SEM, with significance determined by one-way ANOVA compared to the 10-14 week-old group: $*P < 0.05$, $**P < 0.01$, $***P < 0.001$, $****P < 0.0001$. The data of blue dash line in Fig. 5A-5H and 5L, and blue bar in 5J-5K were presented in previous figure, here just used for comparison between non-diabetic group and diabetes group.

Figure 6. A working model for dynamic interactions between alpha and delta cells during autoimmune progression in non-diabetic NOD mice.

Dynamic changes in alpha and delta cell areas in non-diabetic NOD mice across different age groups. The green line indicates the area of alpha cells, the purple line indicates the area of delta cells, the red line represents the area of glucagon and

somatostatin double-positive cells, and the orange line represents the proliferation of delta cells. Before immune cell infiltration, there are sufficient beta cells (CD45+/-Ins+Gcg+Sst+/−) in the pancreas to maintain blood glucose homeostasis. As immune cells infiltrate the pancreas, beta cells are rapidly lost. Based on statistical results, two main types of islets emerge at this stage: one gradually transforms into islets primarily composed of alpha cells (CD45+Ins−Gcg+Sst−), while the other type exhibits a rapid increase in delta cell ratio (CD45+Ins−Gcg+Sst+). As beta cells continue to decrease, the number of immune cells near the islets also diminishes, and the proportion of two types of islets (CD45−Ins−Gcg+Sst− and CD45−Ins−Gcg+Sst+) increases, indicating that these are the final two predominant forms of endocrine cell composition in the islets. Our data suggest that the increased delta cells are not primarily derived from self-proliferation but rather from the transdifferentiation of alpha cells. Some alpha cells first dedifferentiate into endocrine precursor cells (Ngn3+), and then eventually transdifferentiate into delta cells. Moreover, the increased delta cells in the pancreas secrete more somatostatin, which inhibits glucagon secretion by alpha cells and leads to a reduced response to low glucose stimuli.